DMD Fast Forward. Published on October 14, 2010 as doi:10.1124/dmd.110.035287

Activation of the acute inflammatory response alters cytochrome P450 expression and eicosanoid metabolism

Katherine N. Theken, Yangmei Deng, M. Alison Kannon, Tricia M. Miller,

Samuel M. Poloyac, and Craig R. Lee

Division of Pharmacotherapy and Experimental Therapeutics, Eshelman School of Pharmacy, University of North Carolina, Chapel Hill, NC (KNT, YD, MAK, CRL)

Department of Pharmaceutical Sciences, School of Pharmacy, University of Pittsburgh, Pittsburgh, PA (TMM, SMP)

DMD Fast Forward. Published on October 14, 2010 as DOI: 10.1124/dmd.110.035287
This article has not been copyedited and formatted. The final version may differ from this version.

Running title: Endotoxemia alters CYP-mediated eicosanoid metabolism

Corresponding Author: Craig R. Lee, Pharm.D., Ph.D.

2317 Kerr Hall, CB# 7569

Chapel Hill, NC 27599

Phone: (919) 843-7673

Fax: (919) 962-0644

craig_lee@unc.edu

Number of text pages: 32

Number of tables: 0 (1 supplemental table)

Number of figures: 7 (2 supplemental figures)

Number of references: 38

Number of words in abstract: 246

Number of words in introduction: 373

Number of words in discussion: 1498

Nonstandard abbreviations: CYP, cytochrome P450; EET, epoxyeicosatrienoic acid; DHET, dihydroxyeicosatrienoic acid; sEH, soluble epoxide hydrolase; 20-HETE, 20-hydroxyeiocatetraenoic acid; NF-κB, nuclear factor-κB; LPS, lipopolysaccharide; TNF-α, tumor necrosis factor-α; PPAR-α, peroxisome proliferator-activated receptor-α; PXR, pregnane X receptor; Stat-1, signal transducer and activator of transcription-1

DMD Fast Forward. Published on October 14, 2010 as DOI: 10.1124/dmd.110.035287
This article has not been copyedited and formatted. The final version may differ from this version.

Abstract

Cytochrome P450 (CYP)-mediated metabolism of arachidonic acid regulates inflammation in hepatic and extra-hepatic tissue. CYP2C/CYP2J-derived epoxyeicosatrienoic and dihydroxyeicosatrienoic acids (EET+DHET) elicit anti-inflammatory effects, while CYP4A/CYP4F-derived 20-hydroxyeicosatetraenoic acid (20-HETE) is pro-inflammatory. Because the impact of inflammation on CYP-mediated formation of endogenous eicosanoids is unclear, we evaluated CYP mRNA levels and CYP epoxygenase (EET+DHET) and ω-hydroxylase (20-HETE) metabolic activity in liver, kidney, lung, and heart in mice 3, 6, 24, and 48 hours following intraperitoneal lipopolysaccharide (LPS, 1 mg/kg) or saline administration. Hepatic *Cyp2c29*, *Cyp2c44*, and *Cyp2j5* mRNA levels and EET+DHET formation were significantly lower 24 and 48 hours following LPS administration. Hepatic *Cyp4a12a*, *Cyp4a12b*, and *Cyp4f13* mRNA levels and 20-HETE formation were also significantly lower at 24 hours, but recovered to baseline at 48 hours, resulting in a significantly higher 20-HETE:EET+DHET formation rate ratio compared to saline-treated mice. Renal CYP mRNA levels and CYP-mediated eicosanoid metabolism were similarly suppressed 24 hours after LPS treatment. Pulmonary EET+DHET formation was lower at all time points after LPS administration, while 20-HETE formation was suppressed in a time-dependent manner, with the lowest formation rate observed at 24 hours. No differences in EET+DHET or 20-HETE formation were observed in heart. Collectively, these data demonstrate that acute activation of the innate immune response alters CYP expression and eicosanoid metabolism in mice in an isoform-, tissue-, and time-dependent manner. Further study is necessary to determine whether therapeutic restoration of the functional balance between the CYP epoxygenase and ω-hydroxylase pathways is an effective anti-inflammatory strategy.

Introduction

In addition to their role in xenobiotic metabolism, cytochromes P450 (CYP) metabolize numerous endogenous substrates, including steroids, hormones, and fatty acids, to biologically active mediators (Roman, 2002). One such example is the oxidative metabolism of arachidonic acid to epoxyeicosatrienoic acids (EETs) and hydroxyeicosatetraenoic acids (HETEs). Olefin epoxidation of arachidonic acid to four EET regioisomers (5,6-EET, 8,9-EET, 11,12-EET, 14,15-EET) is primarily catalyzed by CYP2C and CYP2J isoforms (Zeldin, 2001). Soluble epoxide hydrolase (sEH, *Ephx2*) rapidly hydrolyzes EETs to dihydroxyeicosatrienoic acids (DHETs), which, in general, are less biologically active. In contrast, ω-hydroxylation of arachidonic acid by CYP4A and CYP4F isoforms produces 20-HETE (Roman, 2002).

EETs and 20-HETE regulate numerous biological processes, including vascular tone, angiogenesis, and the response to ischemia/reperfusion injury (Zeldin, 2001; Roman, 2002; Deng et al., 2010). Accumulating evidence has demonstrated that the CYP epoxygenase and ω-hydroxylase pathways also regulate inflammation. The EETs possess potent anti-inflammatory properties by attenuating cytokine-induced nuclear factor-κB (NF-κB) activation and leukocyte adhesion to the vascular wall (Node et al., 1999). Conversely, 20-HETE activates NF-κB signaling and induces expression of cellular adhesion molecules and cytokines, thereby promoting inflammation (Ishizuka et al., 2008).

Due to the divergent effects of the CYP epoxygenase and ω-hydroxylase pathways in the regulation of inflammation, alterations in the functional balance between these parallel pathways may contribute to the pathogenesis and progression of inflammatory diseases, such as sepsis, cancer, and cardiovascular disease. Although it is well-established that acute inflammatory stimuli suppress hepatic CYP expression via a pretranslational mechanism, thereby decreasing xenobiotic metabolism and clearance in preclinical models and humans (Morgan, 2001; Riddick et al., 2004; Morgan et al., 2008), the effect on CYP-mediated

eicosanoid metabolism in hepatic and extra-hepatic tissue has not been rigorously evaluated. Moreover, the biological properties of the CYP epoxygenase and ω-hydroxylase pathways *in vivo* are most commonly investigated in mouse models; however, the relative expression and function of each pathway across tissues in mice has not been well described to date. Therefore, we sought to characterize the (1) relative expression and metabolic activity of the CYP epoxygenase and ω-hydroxylase pathways across liver, kidney, lung, and heart in mice, and (2) impact of acute inflammation induced by systemic lipopolysaccharide (LPS) administration on CYP epoxygenase and ω-hydroxylase expression and metabolic activity in each tissue.

Methods

Reagents

All reagents were purchased from Fisher Scientific (Pittsburgh, PA, USA) unless otherwise noted.

Experimental Protocol

Male C57Bl/6 mice (4-5 months of age) were treated with *E. coli* LPS (1 mg/kg; serotype O111:B4, 1,000,000 EU/mg; Sigma, St. Louis, MO) or endotoxin-free saline by intraperitoneal injection and were euthanized by CO_2 inhalation 3, 6, 24, or 48 hours after treatment. Liver, kidney, lung, heart and aorta were harvested and flash frozen in liquid nitrogen. Blood was collected in heparinized tubes, and plasma was separated by centrifugation. Tissue and plasma were stored at -80ºC pending analysis. All studies were in accordance with principles outlined in the *NIH Guide for the Care and Use of Laboratory Animals* and were approved by the Institutional Animal Care and Use Committee at the University of North Carolina at Chapel Hill.

RNA isolation, reverse transcription, and qRT-PCR

Total RNA was isolated from whole tissue homogenates using the RNeasy Miniprep Kit (QIAGEN, Valencia, CA) per the manufacturer's instructions. Total RNA was reverse transcribed to cDNA using the ABI High Capacity cDNA Reverse Transcription Kit (Applied Biosystems, Foster City, CA) with a reaction temperature of 25ºC for 10 minutes then 37ºC for 120 minutes. Expression of murine *Cyp2c29*, *Cyp2c44*, *Cyp2j5*, *Cyp2j9*, *Cyp4a12a*, *Cyp4a12b*, *Cyp4f13*, *Cyp4f16*, *Ephx2*, and *GAPDH* were quantified by quantitative RT-PCR using commercially available Taqman® Assays on Demand (Applied Biosystems) (Supplemental Table 1). CYP isoforms were selected based on known epoxygenase or ω-hydroxylase activity and/or expression in several of the tissues examined in an initial expression screen (Luo et al., 1998; Ma et al., 1999; Qu et al., 2001; DeLozier et al., 2004; Wang et al., 2004; Muller et al.,

2007). The metabolic activity of murine Cyp4f isoforms has not been characterized, but these isoforms were included as CYP4F isoforms in other species have been shown to catalyze 20-HETE formation (Powell et al., 1998; Christmas et al., 2001; Xu et al., 2004). Each reaction was carried out in a 20 µL volume with 50 ng cDNA, 20X Assay on Demand, and 2X Taqman® Universal PCR Master Mix. All reactions were performed in triplicate using the ABI Prism 7300 Sequence Detection System. The cycling conditions were as follows: 2 minutes at 50ºC, 10 minutes at 95ºC, and 40 cycles of 15 seconds at 95ºC followed by 60 seconds at 60ºC. The efficiency of each RT-PCR probe was calculated over a range of cDNA amounts (1-100 ng), as previously described (Pfaffl, 2001), and was equivalent for all probes (data not shown). CYP mRNA levels were normalized to *GAPDH* and expressed relative to the saline-treated controls using the $2^{-\Delta\Delta Ct}$ method (Livak and Schmittgen, 2001).

Microsome isolation

Microsomal fractions from liver, kidney, lung, and heart were isolated as previously described (Lee et al., 2007). Briefly, frozen tissue was homogenized in 0.25 M sucrose/10mM Tris-HCl buffer (pH 7.5) containing protease inhibitors. Liver and kidney homogenates were prepared from individual mice. Lung and heart homogenates were prepared from tissue pooled from 2-4 mice, due to the tissue size and low levels of CYP expression. Homogenates were centrifuged at 4ºC at 2570 x *g* for 20 minutes, then at 10300 x *g* for 20 minutes to remove cellular debris. The supernatants were then centrifuged at 100000 x *g* at 4ºC for 90 minutes. The resulting microsomal pellets were resuspended in 50 mM Tris/1 mM DTT/1 mM EDTA buffer (pH 7.5) containing 20% glycerol. Protein concentrations were quantified using the Bio-Rad protein assay (Bio-Rad, Hercules, CA), per the manufacturer's instructions.

Microsomal incubations

Incubations contained 300 µg (liver, kidney) or 350 µg (lung, heart) microsomal protein and 50 µM (liver, kidney, heart) or 150 µM (lung) arachidonic acid in a 1 mL volume of 0.12 M potassium phosphate incubation buffer containing 5 mM magnesium chloride, as previously described (Poloyac et al., 2004). In the presence of these saturating substrate concentrations, formation rates reflect the amount of metabolically active protein (Poloyac et al., 2004). The limited amount of tissue precluded assessment of CYP epoxygenase and ω-hydroxylase activity in aorta. Reactions were initiated by the addition of 1 mM NADPH and were carried out at 37ºC for 20 minutes (liver, kidney) or 60 minutes (lung, heart). In lung and heart incubations, an additional 1 mM NADPH was added after 30 minutes. Incubations were carried out at saturating concentrations of substrate, and metabolite formation was linear with respect to incubation time and microsomal protein, as determined from preliminary incubations. The reactions were stopped by placing the samples on ice, and 12.5 ng 20-HETE-d6 was added as an internal standard. Due to high metabolite formation, liver incubations were diluted 20-fold in incubation buffer prior to addition of internal standard. Metabolites were extracted with diethyl ether, evaporated to dryness under nitrogen gas, and reconstituted in 80% methanol in deionized water for analysis.

UPLC-MS/MS

Arachidonic acid metabolites (14,15-EET, 11,12-EET, 8,9-EET, 14,15-DHET, 11,12-DHET, 8,9-DHET, 5,6-DHET, and 20-HETE) in microsomal incubations and plasma were quantified by UPLC-MS/MS as previously described (Miller et al., 2009). Analytes were separated on a UPLC BEH C-18, 1.7 µm (2.1 mm x 100 mm) reversed-phase column (Waters, Milford, MA) protected by a guard column (2.1 mm x 5 mm; Waters). Mobile phases consisted of 0.005% acetic acid/5% acetonitrile in deionized water (A) and 0.005% acetic acid in acetonitrile (B) at an initial mixture of 65% A and 35% B. Mobile phase B increased from 35% to 70% in a linear gradient over 4 minutes, then increased to 95% over 0.5 minute where it

remained for 0.3 minute. This was followed by a linear return to the initial conditions over 0.1 minute with a 1.5 minute pre-equilibration period prior to the next sample run.

Mass spectrometric analysis was performed with a TSQ Quantum Ultra (Thermo Fisher Scientific, San Jose, CA) triple quadrupole mass spectrometer coupled with heated electrospray ionization (HESI) operated in negative selective reaction monitoring (SRM) mode. Unit resolutions at both Q1 and Q3 were set at 0.70 full width at half maximum. Quantitation by SRM analysis on EETs, DHETs, and HETEs was performed by monitoring their *m/z* transitions. Parameters were optimized to obtain the highest $[M-H]^-$ ion abundance and were as follows: capillary temperature 400ºC, spray voltage 3000V, and a source collision-induced dissociation set at 0V. Sheath gas, auxiliary gas, and ion sweep gas pressures were set at 65, 55, and 3, respectively. Scan time was set at 0.01 seconds and collision gas pressure was set at 1.3 mTorr. Analytical data was acquired and analyzed using Xcaliber software version 2.0.6 (ThermoFinnigan, San Jose, CA). Metabolite concentrations were calculated from a standard curve and expressed as formation rates (pmol/mg protein/min).

Statistical analysis

All data are expressed as mean ± standard error of the mean (SEM). The sum formation rate of all EET and DHET regioisomers was calculated and used as an index of total CYP epoxygenase metabolic activity. The functional balance between the CYP ω-hydroxylase and epoxygenase pathways was assessed by the ratio of 20-HETE to total EET+DHET formation. Because the data were not normally distributed, mRNA and protein levels were transformed to ranks and metabolite formation rates were log-transformed prior to statistical analysis. Data from saline-treated mice at each time point were pooled to create a single control group for statistical comparisons. Data were analyzed by one-way ANOVA followed by post-hoc Dunnett's test for comparison to the pooled saline control group. The relationship between CYP mRNA and protein levels and EET+DHET or 20-HETE formation was evaluated

by Spearman rank correlation. Statistical analysis was performed using SAS software (v.9.1.3, SAS Institute, Cary, NC). $P<0.05$ was considered statistically significant.

Results

Induction of cytokine expression

Systemic LPS administration induced tumor necrosis factor-α (TNF-α) expression in a time-dependent manner in all tissues examined, consistent with acute activation of the innate immune response (Figure 1). The most substantial increase was observed 3 and 6 hours after LPS administration. TNF-α expression decreased over time, but remained significantly elevated compared to saline-treated mice in most tissues at 48 hours.

Liver

All CYP isoforms examined were expressed at high levels in liver, with *Cyp2c29* and *Cyp4a12a* being the most abundant CYP epoxygenase and ω-hydroxylase, respectively (Figure 2A). Hepatic *Cyp2c29* (0.06±0.02), *Cyp2c44* (0.18±0.03), and *Cyp2j5* (0.34±0.06) mRNA levels were markedly suppressed 24 hours after LPS administration (Figure 2B), with partial (*Cyp2c29*: 0.62±0.16; *Cyp2c44*: 0.69±0.22) or full (*Cyp2j5*: 1.00±0.25) restoration of expression to basal levels at 48 hours. Hepatic CYP2C and CYP2J protein expression was also significantly suppressed 24 hours after LPS administration (Supplemental Figure 1, $P<0.05$ versus saline). At 48 hours, CYP2C remained significantly suppressed, but CYP2J expression recovered to near-basal levels. Hepatic *Cyp4a12a* (0.47±0.06), *Cyp4a12b* (0.67±0.06), and *Cyp4f13* (0.59±0.08) mRNA levels were also significantly suppressed, but to a lesser degree, 24 hours after LPS administration, and returned to basal levels by 48 hours (*Cyp4a12a*: 0.79±0.22; *Cyp4a12b*: 1.21±0.37; *Cyp4f13*: 1.02±0.33). In contrast, *Cyp4f16* mRNA levels were significantly higher 24 (4.56±0.62) and 48 hours (2.82±0.81) after LPS administration compared to saline controls (Figure 2C). No significant alterations in CYP4A or CYP4F protein expression were observed (Supplemental Figure 1).

Total hepatic CYP epoxygenase metabolic activity was significantly lower 24 (173.9±15.7 pmol/mg protein/min) and 48 (295.4±18.8 pmol/mg protein/min) hours after LPS

DMD Fast Forward. Published on October 14, 2010 as DOI: 10.1124/dmd.110.035287
This article has not been copyedited and formatted. The final version may differ from this version.

administration, compared to the saline control group (458.2±24.0 pmol/mg protein/min), while no differences were observed at 3 and 6 hours (Figure 2D). Similar results were observed when each EET+DHET regioisomer was evaluated individually (Supplemental Figure 2A). Total CYP epoxygenase metabolic activity was strongly correlated with hepatic *Cyp2c29* (r=0.74, P<0.001), *Cyp2c44* (r=0.65, P<0.001), and *Cyp2j5* (r=0.56, P<0.001) mRNA levels, as well as CYP2C (r=0.50, P=0.006) and CYP2J (r=0.37, P=0.056) protein levels. Compared to saline-treated mice (286.7±11.2 pmol/mg protein/min), 20-HETE formation was also significantly lower 24 hours (180.8±17.8 pmol/mg protein/min) after LPS administration, but returned to basal levels at 48 hours (305.5±11.7 pmol/mg protein/min) (Figure 2D). No significant differences in hepatic 20-HETE formation were observed 3 or 6 hours after LPS administration. 20-HETE formation was significantly correlated with hepatic *Cyp4a12b* mRNA levels (r=0.51, P=0.002).

Kidney

Cyp2j5 and *Cyp4a12a* were the most abundant CYP epoxygenase and ω-hydroxylase in kidney, respectively, while *Cyp2c29* mRNA was undetectable (Figure 3A). Renal *Cyp2c44* mRNA levels were significantly suppressed 3 (0.64±0.06), 6 (0.56±0.03), and 24 hours (0.26±0.03) after LPS administration, but returned to baseline at 48 hours (1.04±0.11). A similar profile was observed for *Cyp2j5*, but *Cyp2j5* was suppressed to a lesser degree (Figure 3B). *Cyp4a12a* expression was also significantly suppressed at 24 hours (0.63±0.06). In contrast, *Cyp4a12b* and *Cyp4f16* mRNA levels were significantly lower at 6 hours, but were significantly higher 24 and 48 hours after LPS administration (Figure 3C, P<0.05 versus saline). Significant changes in *Cyp4f13* mRNA levels were observed only at 24 hours.

Total CYP epoxygenase metabolic activity was significantly lower in kidney microsomes 24 hours (13.2±0.7 pmol/mg protein/min) after LPS administration, compared to the saline control group (18.7±1.6 pmol/mg protein/min). Formation of the 14,15- and 11,12-, but not the 8,9- or 5,6-, regioisomers was significantly lower 24 hours after LPS administration

DMD Fast Forward. Published on October 14, 2010 as DOI: 10.1124/dmd.110.035287
This article has not been copyedited and formatted. The final version may differ from this version.

(Supplemental Figure 2B). At 48 hours, total EET+DHET formation was returning to basal levels (14.7±1.4 pmol/mg protein/min; P=0.12 vs. saline) (Figure 3D). Similarly, renal 20-HETE formation was significantly lower in LPS-treated mice at 24 hours (15.3±1.9 pmol/mg protein/min), compared to saline (32.5±6.7 pmol/mg protein/min), but was recovering toward baseline at 48 hours (22.2±4.9 pmol/mg protein/min; P=0.45 vs. saline) (Figure 3D). No significant differences in renal EET+DHET, or 20-HETE formation were observed 3 or 6 hours after LPS administration. A significant correlation between total CYP epoxygenase and ω-hydroxylase metabolic activity, and renal *Cyp2j5* (r=0.42, P=0.012) and *Cyp4a12a* mRNA levels (r=0.55, P<0.001), respectively, was observed.

Lung

Cyp2j9 was the most abundant CYP epoxygenase isoform expressed in lung (Figure 4A). *Cyp2j9* and *Cyp2c44* mRNA levels were significantly lower in LPS-treated mice at 3, 6, 24, and 48 hours (Figure 4B, P<0.05 versus saline). *Cyp2j5* also appeared to be suppressed at 24 hours (0.20±0.05; P=0.11); however, due to substantial inter-animal variability, these differences were not statistically significant (Figure 4B). Following LPS administration, *Cyp4a12a*, *Cyp4a12b*, *Cyp4f13*, and *Cyp4f16* mRNA levels were significantly lower at almost every time point, although *Cyp4f16* returned to basal levels at 48 hours (Figure 4C).

Compared to saline-treated mice (54.1±5.2 pmol/mg protein/min), total CYP epoxygenase metabolic activity in lung microsomes was lower, but not statistically significant, 3 (35.8±3.0 pmol/mg protein/min, P=0.063), 6 (38.4±7.3 pmol/mg protein/min, P=0.171), and 24 (38.7±3.7 pmol/mg protein/min, P=0.094) hours after LPS treatment, while EET+DHET formation was significantly lower at the 48 hour time point (28.9±2.2 pmol/mg protein/min, P=0.008) (Figure 4D). Similar time-dependent changes in metabolism were observed for each regioisomer (Supplemental Figure 2C). 20-HETE formation was significantly lower 6 (12.8±5.9 pmol/mg protein/min) and 24 (9.4±1.5 pmol/mg protein/min) hours after LPS administration,

DMD Fast Forward. Published on October 14, 2010 as DOI: 10.1124/dmd.110.035287
This article has not been copyedited and formatted. The final version may differ from this version.

compared to the saline control group (23.1±1.4 pmol/mg protein/min), whereas no differences were observed at 3 or 48 hours (Figure 4D). No significant correlations between total CYP epoxygenase metabolic activity and *Cyp2c44*, *Cyp2j5*, or *Cyp2j9* mRNA levels were observed. However, 20-HETE formation significantly correlated with pulmonary *Cyp4a12a* (r=0.47, P=0.026), *Cyp4a12b* (r=0.46, P=0.030), and *Cyp4f13* (r=0.46, P=0.033) mRNA levels.

Heart/Aorta

Overall, myocardial CYP mRNA levels were low, with *Cyp4f13* and *Cyp4f16* being the most abundant isoforms. Of the CYP epoxygenases examined, only *Cyp2c44* was expressed at detectable levels (Figure 5A). The CYP expression profile in aorta was similar; however, *Cyp2c29* mRNA was expressed at detectable levels, and *Cyp2c44* and *Cyp4f13* mRNA levels were approximately 10-fold higher in aorta compared to heart (Supplemental Table 1). Myocardial *Cyp2c44* mRNA levels were significantly lower 3 and 6 hours after LPS administration (Figure 5B, P<0.05 versus saline). Although it remained significantly suppressed at 24 hours (0.51±0.14), *Cyp2c44* appeared to be returning to basal levels, with full recovery observed at 48 hours (0.78 ±0.13). In aorta, *Cyp2c29* (0.38±0.12, P=0.128) and *Cyp2c44* (0.26±0.06, P=0.128) mRNA appeared to be suppressed 24 hours after LPS administration, relative to saline-treated mice, but this difference was not statistically significant due to substantial inter-animal variability. In heart, both *Cyp4f13* and *Cyp4f16* mRNA levels were significantly lower in LPS-treated mice at 3 hours, but significantly higher at 24 and 48 hours (Figure 5C, P<0.05 versus saline). Similarly, *Cyp4f13* and *Cyp4f16* mRNA levels in aorta were significantly higher in LPS-treated mice at 24 (*Cyp4f13*: 1.48±0.12; *Cyp4f16*: 3.65±0.44; P<0.05 vs. saline) and 48 hours (*Cyp4f13*: 1.93±0.18; *Cyp4f16*: 3.30±0.61; P<0.05 vs. saline).

Total CYP epoxygenase metabolic activity (3.97±0.44 pmol/mg protein/min) was approximately 8-fold higher than CYP ω-hydroxylase activity (0.51±0.04 pmol/mg protein/min) in heart microsomes under basal conditions (Figure 5D). Compared to saline, no significant

differences in EET+DHET or 20-HETE formation were observed 24 hours after LPS administration. Although EET+DHET formation appeared to be lower and 20-HETE formation appeared to be higher 48 hours after LPS administration, the limited sample size (N=2 incubations) at 48 hours precluded statistical comparisons.

Ephx2 expression

Ephx2 was abundantly expressed in all tissues examined. In liver, kidney, and lung, *Ephx2* mRNA levels were similar to the CYP isoforms examined. In contrast, *Ephx2* was approximately 100- and 10-fold more abundant than *Cyp4f13* in heart and aorta, respectively (Supplemental Table 1). Tissue-specific alterations in *Ephx2* expression were observed following LPS administration (Figure 6). In liver, kidney, and lung, *Ephx2* expression was suppressed by 30-80% 6 to 48 hours following LPS administration, relative to saline control. In contrast, no differences were observed in heart, and *Ephx2* mRNA levels were significantly higher in aorta at 48 hours (2.57±0.49, $P<0.05$ vs. saline).

Functional balance between CYP epoxygenase and ω-hydroxylase pathways across tissues

Under basal conditions, hepatic EET+DHET formation was higher than 20-HETE formation, resulting in a 20-HETE: EET+DHET formation rate ratio of 0.64±0.03 in saline-treated mice (Figure 7A). A similar 20-HETE: EET+DHET formation rate ratio was observed in lung (0.45±0.06, Figure 7C) and heart (0.13±0.02, Figure 7D), indicative of higher CYP epoxygenase metabolic activity relative to CYP ω-hydroxylase metabolic activity. In contrast, the renal ratio of CYP ω-hydroxylase to CYP epoxygenase metabolic activity was 1.69±0.25 (Figure 7B), due to higher 20-HETE compared to EET+DHET formation under basal conditions in kidney.

Following LPS stimulation, the hepatic 20-HETE: EET+DHET formation rate ratio was significantly greater at 24 (1.02±0.06) and 48 (1.05±0.06) hours compared to saline-treated mice (Figure 7A). Although the ratio of CYP ω-hydroxylase to CYP epoxygenase metabolic

activity in heart appeared higher 48 hours after LPS treatment (0.23±0.06), the limited sample size precluded formal statistical comparisons (Figure 7D). In contrast, the pulmonary 20-HETE: EET+DHET formation rate ratio was significantly lower at 24 hours (0.24±0.02) compared to saline-treated mice (Figure 7C). In kidney, no significant differences in the ratio of CYP ω-hydroxylase to CYP epoxygenase metabolic activity were observed after LPS treatment (Figure 7B), which remained greater than 1.0 at all time-points.

Compared to saline-treated mice, plasma 14,15-DHET levels were significantly higher 6 hours after LPS administration; however, no differences in DHET levels were observed at 3, 24 or 48 hours (Supplemental Figure 2E). Plasma EETs and 20-HETE were below the limit of detection in the majority of mice (data not shown).

Discussion

Although it is well established that acute inflammatory stimuli suppress hepatic CYP expression and xenobiotic metabolism, the effect on CYP-mediated eicosanoid metabolism in hepatic and extra-hepatic tissues has not been characterized to date. To our knowledge, this is the first study demonstrating that acute activation of the innate immune response alters CYP epoxygenase and ω-hydroxylase metabolic activity in mice, through pretranslational regulation of CYP expression, and disrupts the functional balance between these parallel pathways in a tissue- and time-dependent manner. Collectively, these findings suggest that alteration of CYP-mediated eicosanoid metabolism is an important consequence of the acute inflammatory response *in vivo*.

Under basal conditions, CYP epoxygenase and ω-hydroxylase metabolic activity in liver was approximately 10-20-fold greater than kidney and lung, and 100-fold greater than heart. In contrast to the other tissues examined, CYP mRNA levels in heart and aorta were low, with *Cyp4f13* and *Cyp4f16* being the most abundant isoforms. Myocardial EET+DHET formation was approximately 8-fold higher than 20-HETE formation despite the high levels of *Cyp4f13* and *Cyp4f16*, suggesting that these isoforms play a minor role in 20-HETE biosynthesis.

Consistent with previous studies in human hepatocyte culture (Abdel-Razzak et al., 1993) and in rodents (Sewer et al., 1996; Barclay et al., 1999), hepatic CYP epoxygenase mRNA, protein, and metabolic activity was suppressed 24 hours after LPS treatment, with partial (CYP2C) or full (CYP2J) restoration to basal levels at 48 hours. The correlation between time-dependent changes in hepatic *Cyp2c29*, *Cyp2c44*, and *Cyp2j5* mRNA levels and epoxygenase metabolic activity support the hypothesis that inflammation-mediated alterations in CYP metabolism are mediated primarily via pretranslational regulation of CYP expression (Morgan et al., 2008). Although Cyp2c29, Cyp2c44, and Cyp2j5 catalyze the formation of individual EET regioisomers in different proportions (Luo et al., 1998; Ma et al., 1999; DeLozier

et al., 2004), the collective suppression of all EET+DHET regioisomers is consistent with the regioisomer profiles for these isoforms.

In contrast to the majority of CYPs, hepatic CYP4A and CYP4F isoforms may be induced by inflammation, although this appears to be isoform- and species-specific (Sewer et al., 1996; Barclay et al., 1999; Kalsotra et al., 2003; Anwar-Mohamed et al., 2010). The temporal profiles of hepatic *Cyp4a12a*, *Cyp4a12b*, and *Cyp4f13* mRNA levels were similar to 20-HETE formation, which was also suppressed at 24 hours, but to a lesser degree than EET+DHET formation. The significantly higher 20-HETE:EET+DHET formation rate ratio at 24 and 48 hours suggests that following systemic activation of the innate immune response, the functional balance in liver is tipped in favor of the pro-inflammatory CYP ω-hydroxylase pathway.

Consistent with previous findings in rats (Anwar-Mohamed et al., 2010), LPS suppressed renal *Cyp2c44* and *Cyp2j5* expression and epoxygenase metabolic activity, which correlated with *Cyp2j5* mRNA levels. This suggests a pretranslational mechanism and that Cyp2j5 is primarily responsible for renal EET formation. We observed lower *Cyp4a12a*, but higher *Cyp4a12b*, *Cyp4f13*, and *Cyp4f16* mRNA levels in kidney following LPS administration. Renal *Cyp4a10* mRNA levels were also higher 24 and 48 hours after LPS administration (data not shown), which is consistent with previous reports (Barclay et al., 1999). However, Cyp4a10 does not readily catalyze 20-HETE formation (Muller et al., 2007). Renal CYP ω-hydroxylase activity was suppressed at 24 hours and significantly correlated with *Cyp4a12a* mRNA levels, suggesting that Cyp4a12a is primarily responsible for renal 20-HETE formation. In contrast to the other tissues examined, CYP ω-hydroxylase metabolic activity predominated under both basal and LPS-stimulated conditions, indicating that inhibition of 20-HETE biosynthesis may be a rational therapeutic strategy to attenuate renal inflammation.

In lung, our findings are consistent with studies demonstrating lower pulmonary CYP2C and CYP2J expression and epoxygenase metabolic activity in rat models of sepsis (Cui et al., 2004) and *Pseudomonas* pneumonia (Yaghi et al., 2003; Yaghi et al., 2004), providing further evidence that suppression of pulmonary EET formation is a key component of the pathological response to inflammation. Compared to basal conditions, 20-HETE formation and the 20-HETE:EET+DHET formation rate ratio were significantly lower 24 hours after LPS administration, suggesting that the functional balance was shifted in favor of the anti-inflammatory CYP epoxygenase pathway. Although this could serve as a compensatory mechanism to facilitate resolution of the inflammatory response, additional studies are necessary to dissect the role of CYP-mediated EET and 20-HETE biosynthesis in the regulation of pulmonary inflammation.

A recent study demonstrated that myocardial CYP epoxygenase activity was significantly suppressed, while CYP ω-hydroxylase activity was induced following LPS administration in rats (Anwar-Mohamed et al., 2010). Although we observed no significant changes in CYP epoxygenase or ω-hydroxylase metabolic activity, the low arachidonic acid-metabolizing capacity of mouse heart limited our sample size. Future studies remain necessary to characterize the effect of inflammation on myocardial CYP epoxygenase and ω-hydroxylase metabolic activity.

Plasma EETs and 20-HETE were below the limit of detection in the majority of mice, consistent with previous reports (Schmelzer et al., 2005; Kubala et al., 2010). Plasma DHET levels appeared modestly elevated 6 hours after LPS administration, consistent with previous studies (Schmelzer et al., 2005; Fife et al., 2008; Kubala et al., 2010); however, only 14,15-DHET was statistically significant. Importantly, the primary source of circulating EET, DHET, and 20-HETE levels in plasma has not been determined. A recent study demonstrated that LPS-induced elevations in plasma DHETs were attenuated in myeloperoxidase-deficient (*Mpo*$^{-/-}$)

mice, suggesting that lipid peroxidation by reactive oxygen species may serve as a CYP-independent source of circulating eicosanoids (Kubala et al., 2010). Furthermore, since EETs and 20-HETE circulate at levels <1.0 ng/mL, it has been hypothesized that these mediators act predominantly in a paracrine manner (Roman, 2002). Our data demonstrate that systemic activation of the innate immune response significantly alters the formation of EETs and 20-HETE in tissue. Future studies characterizing the functional consequences of these local effects remain necessary.

It is believed that the primary mechanism by which CYP expression is down-regulated in response to LPS is cytokine-mediated suppression of gene transcription. However, identification of the specific nuclear receptors that mediate these effects has remained elusive (Morgan, 2001; Riddick et al., 2004; Morgan et al., 2008). For example, an initial study suggested that LPS-mediated alteration of hepatic and renal CYP expression was mediated by peroxisome proliferator-activated receptor-α (PPAR-α) (Barclay et al., 1999). However, subsequent experiments have demonstrated that LPS-mediated down-regulation of hepatic CYP expression is independent of PPAR-α, pregnane X receptor (PXR), and signal transducer and activator of transcription (Stat)-1 (Pan et al., 2003; Richardson and Morgan, 2005). Although we did not directly investigate the mechanism by which LPS alters CYP expression and metabolic activity, the observed isoform- and tissue-specific response suggests that the mechanism is complex, and most likely involves multiple transcription factors that vary across isoforms and tissues. Moreover, the time-dependent changes observed further suggest a multi-factorial mechanism. In addition, multiple murine CYP isoforms catalyze EET and 20-HETE formation, further complicating the ability to identify a single factor that underlies the net impact of the inflammatory response on CYP-mediated eicosanoid metabolism in each tissue. Future studies remain necessary to dissect these complex mechanisms.

CYP-derived EETs possess anti-inflammatory properties via inhibition of NF-κB activation (Node et al., 1999), while 20-HETE activates NF-κB signaling and elicits pro-

inflammatory effects (Ishizuka et al., 2008). These opposing effects on the regulation of inflammation suggest that inflammation-induced alterations in the functional balance between these parallel pathways may contribute to the pathologic consequences of the inflammatory response. A limitation of the current work is that we did not directly demonstrate that potentiation of the CYP epoxygenase pathway and/or inhibition of the CYP ω-hydroxylase pathway attenuates the acute inflammatory response to LPS in each tissue. However, our findings provide an important foundation to guide future studies evaluating these therapeutic strategies, particularly in tissues where inflammatory stimuli tip the functional balance in favor of CYP-mediated 20-HETE biosynthesis, such as liver. Indeed, the liver is the predominant source of cytokine production and drives the systemic inflammatory response, as observed during sepsis, via subsequent activation of extra-hepatic inflammation and multi-organ dysfunction (Szabo et al., 2002). Inhibition of sEH-mediated EET hydrolysis has potent anti-inflammatory effects, including attenuation of endotoxemia-induced hypotension and mortality (Schmelzer et al., 2005; Luria et al., 2007; Liu et al., 2009). In contrast, a recent study demonstrated that LPS-induced hepatic inflammation was not attenuated in *Ephx2*$^{-/-}$ mice or by sEH inhibition (Fife et al., 2008). Although the mechanisms underlying these conflicting findings remain unclear, our data suggest that dual inhibition of 20-HETE biosynthesis and sEH-mediated EET hydrolysis may be a more effective means to attenuate hepatic inflammation. Future studies remain necessary to evaluate these therapeutic strategies in disease models of local and systemic inflammation.

In conclusion, our findings demonstrate that acute activation of the inflammatory response with LPS alters CYP epoxygenase and ω-hydroxylase expression and metabolic activity in a tissue-, isoform-, and time-dependent manner. These results highlight the relative differences in CYP-mediated eicosanoid metabolism across tissues under basal and inflammatory conditions, and lay an important foundation to guide future studies that seek to

determine whether therapeutic restoration of the functional balance between the CYP epoxygenase and ω-hydroxylase pathways is an effective anti-inflammatory strategy *in vivo*.

Authorship Contribution

Participated in research design: Theken, Deng, Poloyac, and Lee.
Conducted experiments: Theken, Deng, Kannon, and Miller.
Contributed new reagents or analytic tools: Miller and Poloyac.
Performed data analysis: Theken and Lee.
Wrote or contributed to the writing of the manuscript: Theken, Poloyac, and Lee.
Other: Theken, Poloyac, and Lee acquired funding for the research.

References

Abdel-Razzak Z, Loyer P, Fautrel A, Gautier JC, Corcos L, Turlin B, Beaune P and Guillouzo A (1993) Cytokines down-regulate expression of major cytochrome P-450 enzymes in adult human hepatocytes in primary culture. *Mol Pharmacol* **44:**707-715.

Anwar-Mohamed A, Zordoky BN, Aboutabl ME and El-Kadi AO (2010) Alteration of cardiac cytochrome P450-mediated arachidonic acid metabolism in response to lipopolysaccharide-induced acute systemic inflammation. *Pharmacol Res* **61:**410-418.

Barclay TB, Peters JM, Sewer MB, Ferrari L, Gonzalez FJ and Morgan ET (1999) Modulation of cytochrome P-450 gene expression in endotoxemic mice is tissue specific and peroxisome proliferator-activated receptor-alpha dependent. *J Pharmacol Exp Ther* **290:**1250-1257.

Christmas P, Jones JP, Patten CJ, Rock DA, Zheng Y, Cheng SM, Weber BM, Carlesso N, Scadden DT, Rettie AE and Soberman RJ (2001) Alternative splicing determines the function of CYP4F3 by switching substrate specificity. *J Biol Chem* **276:**38166-38172.

Cui X, Wu R, Zhou M, Simms HH and Wang P (2004) Differential expression of cytochrome P450 isoforms in the lungs of septic animals. *Crit Care Med* **32:**1186-1191.

DeLozier TC, Tsao CC, Coulter SJ, Foley J, Bradbury JA, Zeldin DC and Goldstein JA (2004) CYP2C44, a new murine CYP2C that metabolizes arachidonic acid to unique stereospecific products. *J Pharmacol Exp Ther* **310:**845-854.

Deng Y, Theken KN and Lee CR (2010) Cytochrome P450 epoxygenases, soluble epoxide hydrolase, and the regulation of cardiovascular inflammation. *J Mol Cell Cardiol* **48:**331-341.

Fife KL, Liu Y, Schmelzer KR, Tsai HJ, Kim IH, Morisseau C, Hammock BD and Kroetz DL (2008) Inhibition of soluble epoxide hydrolase does not protect against endotoxin-mediated hepatic inflammation. *J Pharmacol Exp Ther* **327:**707-715.

Ishizuka T, Cheng J, Singh H, Vitto MD, Manthati VL, Falck JR and Laniado-Schwartzman M (2008) 20-Hydroxyeicosatetraenoic acid stimulates nuclear factor-kappaB activation and the production of inflammatory cytokines in human endothelial cells. *J Pharmacol Exp Ther* **324:**103-110.

Kalsotra A, Cui X, Antonovic L, Robida AM, Morgan ET and Strobel HW (2003) Inflammatory prompts produce isoform-specific changes in the expression of leukotriene B(4) omega-hydroxylases in rat liver and kidney. *FEBS Lett* **555:**236-242.

Kubala L, Schmelzer KR, Klinke A, Kolarova H, Baldus S, Hammock BD and Eiserich JP (2010) Modulation of arachidonic and linoleic acid metabolites in myeloperoxidase-deficient mice during acute inflammation. *Free Radic Biol Med* **48:**1311-1320.

Lee CR, Bottone FG, Jr., Krahn JM, Li L, Mohrenweiser HW, Cook ME, Petrovich RM, Bell DA, Eling TE and Zeldin DC (2007) Identification and functional characterization of polymorphisms in human cyclooxygenase-1 (PTGS1). *Pharmacogenet Genomics* **17:**145-160.

Liu JY, Tsai HJ, Hwang SH, Jones PD, Morisseau C and Hammock BD (2009) Pharmacokinetic optimization of four soluble epoxide hydrolase inhibitors for use in a murine model of inflammation. *Br J Pharmacol* **156:**284-296.

Livak KJ and Schmittgen TD (2001) Analysis of relative gene expression data using real-time quantitative PCR and the 2(-Delta Delta C(T)) Method. *Methods* **25:**402-408.

Luo G, Zeldin DC, Blaisdell JA, Hodgson E and Goldstein JA (1998) Cloning and expression of murine CYP2Cs and their ability to metabolize arachidonic acid. *Arch Biochem Biophys* **357:**45-57.

Luria A, Weldon SM, Kabcenell AK, Ingraham RH, Matera D, Jiang H, Gill R, Morisseau C, Newman JW and Hammock BD (2007) Compensatory mechanism for homeostatic blood pressure regulation in Ephx2 gene-disrupted mice. *J Biol Chem* **282:**2891-2898.

Ma J, Qu W, Scarborough PE, Tomer KB, Moomaw CR, Maronpot R, Davis LS, Breyer MD and Zeldin DC (1999) Molecular cloning, enzymatic characterization, developmental expression, and cellular localization of a mouse cytochrome P450 highly expressed in kidney. *J Biol Chem* **274:**17777-17788.

Miller TM, Donnelly MK, Crago EA, Roman DM, Sherwood PR, Horowitz MB and Poloyac SM (2009) Rapid, simultaneous quantitation of mono and dioxygenated metabolites of arachidonic acid in human CSF and rat brain. *J Chromatogr B Analyt Technol Biomed Life Sci* **877:**3991-4000.

Morgan ET (2001) Regulation of cytochrome p450 by inflammatory mediators: why and how? *Drug Metab Dispos* **29:**207-212.

Morgan ET, Goralski KB, Piquette-Miller M, Renton KW, Robertson GR, Chaluvadi MR, Charles KA, Clarke SJ, Kacevska M, Liddle C, Richardson TA, Sharma R and Sinal CJ (2008) Regulation of drug-metabolizing enzymes and transporters in infection, inflammation, and cancer. *Drug Metab Dispos* **36:**205-216.

Muller DN, Schmidt C, Barbosa-Sicard E, Wellner M, Gross V, Hercule H, Markovic M, Honeck H, Luft FC and Schunck WH (2007) Mouse Cyp4a isoforms: enzymatic properties, gender- and strain-specific expression, and role in renal 20-hydroxyeicosatetraenoic acid formation. *Biochem J* **403:**109-118.

Node K, Huo Y, Ruan X, Yang B, Spiecker M, Ley K, Zeldin DC and Liao JK (1999) Anti-inflammatory properties of cytochrome P450 epoxygenase-derived eicosanoids. *Science* **285:**1276-1279.

Pan J, Xiang Q, Ball S, Scatina J, Kao J and Hong JY (2003) Lipopolysaccharide-mediated modulation of cytochromes P450 in Stat1 null mice. *Drug Metab Dispos* **31:**392-397.

Pfaffl MW (2001) A new mathematical model for relative quantification in real-time RT-PCR. *Nucleic Acids Res* **29:**e45.

Poloyac SM, Tortorici MA, Przychodzin DI, Reynolds RB, Xie W, Frye RF and Zemaitis MA (2004) The effect of isoniazid on CYP2E1- and CYP4A-mediated hydroxylation of arachidonic acid in the rat liver and kidney. *Drug Metab Dispos* **32:**727-733.

Powell PK, Wolf I, Jin R and Lasker JM (1998) Metabolism of arachidonic acid to 20-hydroxy-5,8,11, 14-eicosatetraenoic acid by P450 enzymes in human liver: involvement of CYP4F2 and CYP4A11. *J Pharmacol Exp Ther* **285:**1327-1336.

Qu W, Bradbury JA, Tsao CC, Maronpot R, Harry GJ, Parker CE, Davis LS, Breyer MD, Waalkes MP, Falck JR, Chen J, Rosenberg RL and Zeldin DC (2001) Cytochrome P450 CYP2J9, a new mouse arachidonic acid omega-1 hydroxylase predominantly expressed in brain. *J Biol Chem* **276:**25467-25479.

Richardson TA and Morgan ET (2005) Hepatic cytochrome P450 gene regulation during endotoxin-induced inflammation in nuclear receptor knockout mice. *J Pharmacol Exp Ther* **314:**703-709.

Riddick DS, Lee C, Bhathena A, Timsit YE, Cheng PY, Morgan ET, Prough RA, Ripp SL, Miller KK, Jahan A and Chiang JY (2004) Transcriptional suppression of cytochrome P450 genes by endogenous and exogenous chemicals. *Drug Metab Dispos* **32:**367-375.

Roman RJ (2002) P-450 metabolites of arachidonic acid in the control of cardiovascular function. *Physiol Rev* **82:**131-185.

Schmelzer KR, Kubala L, Newman JW, Kim IH, Eiserich JP and Hammock BD (2005) Soluble epoxide hydrolase is a therapeutic target for acute inflammation. *Proc Natl Acad Sci U S A* **102:**9772-9777.

Sewer MB, Koop DR and Morgan ET (1996) Endotoxemia in rats is associated with induction of the P4504A subfamily and suppression of several other forms of cytochrome P450. *Drug Metab Dispos* **24:**401-407.

Szabo G, Romics L, Jr. and Frendl G (2002) Liver in sepsis and systemic inflammatory response syndrome. *Clin Liver Dis* **6:**1045-1066.

Wang H, Zhao Y, Bradbury JA, Graves JP, Foley J, Blaisdell JA, Goldstein JA and Zeldin DC (2004) Cloning, expression, and characterization of three new mouse cytochrome p450 enzymes and partial characterization of their fatty acid oxidation activities. *Mol Pharmacol* **65:**1148-1158.

Xu F, Falck JR, Ortiz de Montellano PR and Kroetz DL (2004) Catalytic activity and isoform-specific inhibition of rat cytochrome p450 4F enzymes. *J Pharmacol Exp Ther* **308:**887-895.

Yaghi A, Bend JR, Webb CD, Zeldin DC, Weicker S, Mehta S and McCormack DG (2004) Excess nitric oxide decreases cytochrome P-450 2J4 content and P-450-dependent arachidonic acid metabolism in lungs of rats with acute pneumonia. *Am J Physiol Lung Cell Mol Physiol* **286:**L1260-1267.

Yaghi A, Bradbury JA, Zeldin DC, Mehta S, Bend JR and McCormack DG (2003) Pulmonary cytochrome P-450 2J4 is reduced in a rat model of acute Pseudomonas pneumonia. *Am J Physiol Lung Cell Mol Physiol* **285:**L1099-1105.

Zeldin DC (2001) Epoxygenase pathways of arachidonic acid metabolism. *J Biol Chem* **276:**36059-36062.

Footnotes

This work was supported by a predoctoral fellowship from the American Foundation for Pharmaceutical Education, grants from the National Institutes of Health National Institute of Neurological Disorders and Stroke [Grant R01NS052315] and National Center of Research Resources [Grant S10RR023461], and grants from the University of North Carolina at Chapel Hill [Junior Faculty Development Award], the American Heart Association [Beginning Grant-in-Aid] and the National Institutes of Health National Institute of General Medical Sciences [Grant R01GM088199]. The content is solely the responsibility of the authors and does not necessarily represent the official views of the NIGMS, NINDS or NIH.

DMD Fast Forward. Published on October 14, 2010 as DOI: 10.1124/dmd.110.035287
This article has not been copyedited and formatted. The final version may differ from this version.

Figure Legends

Figure 1: Effect of LPS administration (1 mg/kg, IP) on TNF-α mRNA levels over 48 hours in liver, kidney, lung, heart, and aorta. Data are expressed as mean ± SEM-fold change in expression, relative to the saline control group, using the $2^{-\Delta\Delta Ct}$ method. N=5-6 per time point.
* P<0.05 versus saline control group.

Figure 2: (A) The relative abundance of hepatic CYP mRNA was quantified in saline-treated mice (N=20) and normalized to *GAPDH*. The time-dependent effect of LPS administration (1 mg/kg, IP) on hepatic (B) *Cyp2c29*, *Cyp2c44*, and *Cyp2j5* and (C) *Cyp4a12a*, *Cyp4a12b*, *Cyp4f13*, and *Cyp4f16* mRNA levels were quantified by qRT-PCR and expressed relative to the saline control group [Saline (pooled): N=20; LPS 3 hours: N=6, 6 hours: N=6, 24 hours: N=15, 48 hours: N=6]. The effect of LPS administration on (D) total CYP epoxygenase (EETs+DHETs) and ω-hydroxylase (20-HETE) metabolic activity in liver microsomes was determined [Saline (pooled): N=12; LPS 3 hours: N=4, 6 hours: N=4, 24 hours: N=12, 48 hours: N=6]. * P<0.05 versus saline control group.

Figure 3: (A) The relative abundance of renal CYP mRNA was quantified in saline-treated mice (N.D.: not detected; N=20 for detected isoforms; N=3 for undetectable isoforms) and normalized to *GAPDH*. The time-dependent effect of LPS administration (1 mg/kg, IP) on renal (B) *Cyp2c44* and *Cyp2j5* and (C) *Cyp4a12a*, *Cyp4a12b*, *Cyp4f13*, and *Cyp4f16* mRNA levels were quantified by qRT-PCR and expressed relative to the saline control group [Saline (pooled): N=20; LPS 3 hours: N=6, 6 hours: N=6, 24 hours: N=15, 48 hours: N=6]. The effect of LPS administration on (D) total CYP epoxygenase (EETs+DHETs) and ω-hydroxylase (20-HETE) metabolic activity in kidney microsomes was determined [Saline (pooled): N=9; LPS 3 hours: N=6, 6 hours: N=6, 24 hours: N=9, 48 hours: N=6]. * P<0.05 versus saline control group.

DMD Fast Forward. Published on October 14, 2010 as DOI: 10.1124/dmd.110.035287
This article has not been copyedited and formatted. The final version may differ from this version.

Figure 4: (A) The relative abundance of pulmonary CYP mRNA was quantified in saline-treated mice (N.D.: not detected; N=23 for detected isoforms; N=3 for undetectable isoforms) and normalized to *GAPDH*. The time-dependent effect of LPS administration (1 mg/kg, IP) on pulmonary (B) *Cyp2c44*, *Cyp2j5*, and *Cyp2j9* and (C) *Cyp4a12a*, *Cyp4a12b*, *Cyp4f13*, and *Cyp4f16* mRNA levels were quantified by qRT-PCR and expressed relative to the saline control group [Saline (pooled): N=23; LPS 3 hours: N=9, 6 hours: N=9, 24 hours: N=18, 48 hours: N=6]. The effect of LPS administration on (D) total CYP epoxygenase (EETs+DHETs) and ω-hydroxylase (20-HETE) metabolic activity in lung microsomes (N=2 mice per microsome preparation) was determined [Saline (pooled): N=6, LPS 3 hours: N=4, 6 hours: N=3, 24 hours: N=6, 48 hours: N=3]. * $P<0.05$ versus saline control group.

Figure 5: (A) The relative abundance of myocardial CYP mRNA was quantified in saline-treated mice (N.D.: not detected; N=24 for detected isoforms; N=3 for undetectable isoforms) and normalized to *GAPDH*. The time-dependent effect of LPS administration (1 mg/kg, IP) on myocardial (B) *Cyp2c44* and (C) *Cyp4f13* and *Cyp4f16* mRNA levels were quantified by qRT-PCR and expressed relative to the saline control group [Saline (pooled): N=24; LPS 3 hours: N=9, 6 hours: N=9, 24 hours: N=18, 48 hours: N=6]. The effect of LPS administration on (D) total CYP epoxygenase (EETs+DHETs) and ω-hydroxylase (20-HETE) metabolic activity in heart microsomes (N=3-4 mice per microsome preparation) was determined [Saline (pooled): N=4; LPS 24 hours: N=4, 48 hours: N=2). * $P<0.05$ versus saline control group.

Figure 6: The time-dependent effect of LPS administration (1 mg/kg, IP) on *Ephx2* mRNA levels in liver, kidney, lung, heart, and aorta were quantified by qRT-PCR and expressed relative to the saline control group [Saline (pooled): N=18-24; LPS 3 hours: N=6-9, 6 hours: N=6-9, 24 hours: N=15-18, 48 hours: N=6]. * $P<0.05$ versus saline control group.

Figure 7: The time-dependent effect of LPS administration (1 mg/kg, IP) on the ratio of 20-HETE to EET+DHET formation was determined in (A) liver, (B) kidney, (C) lung, and (D) heart microsomes. Saline: N=4-12; LPS 3 hours: N=4-6, 6 hours: N=3-6, 24 hours: N=4-12, 48 hours: N=2-6. * $P<0.05$ compared to saline-treated mice.

Figure 1

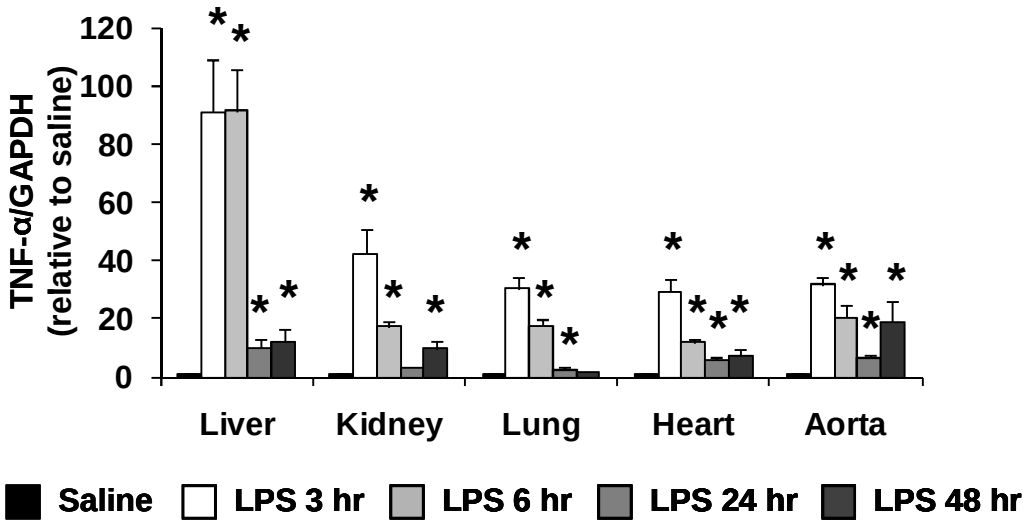

Figure 2: Liver

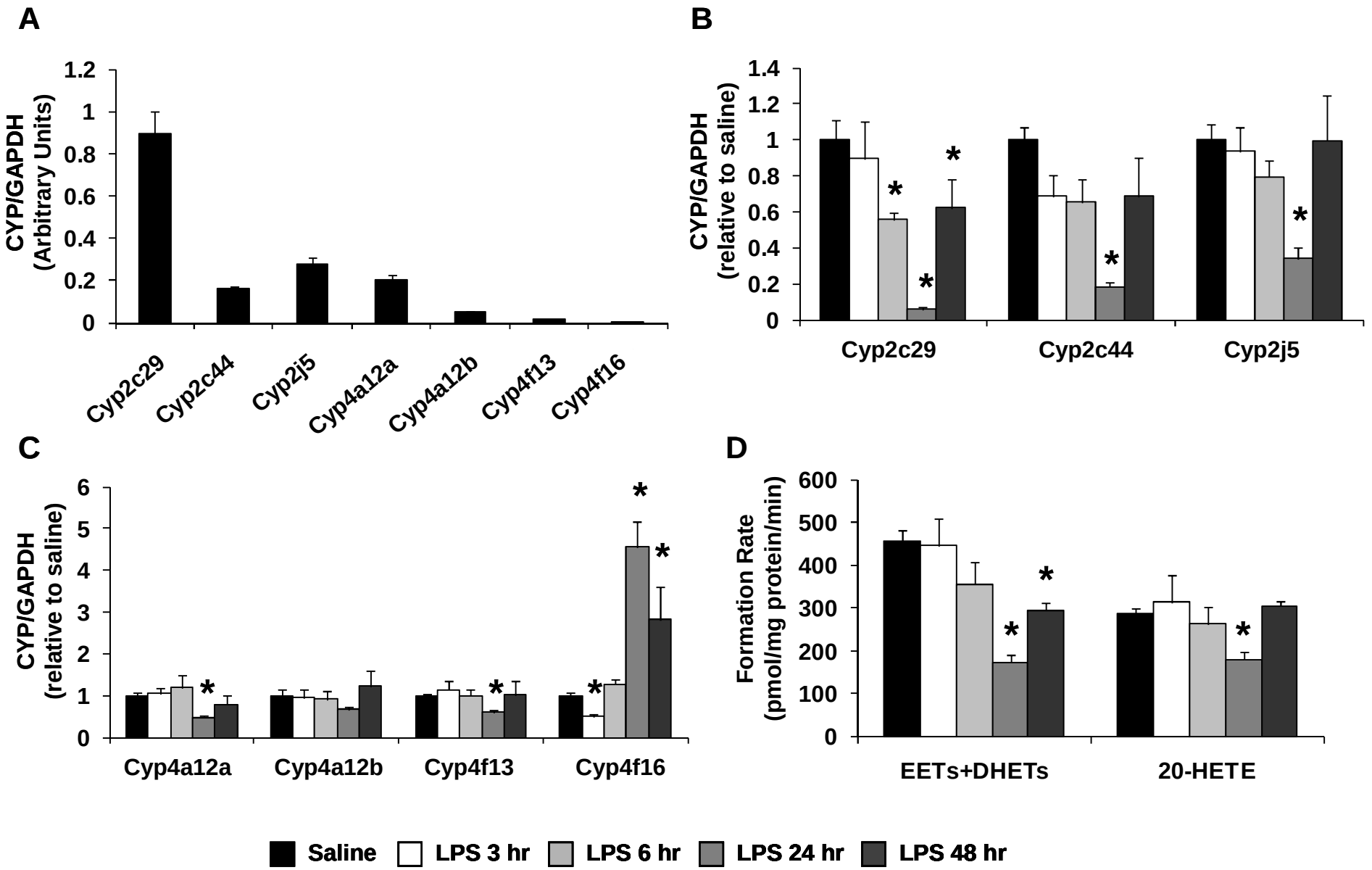

Figure 3: Kidney

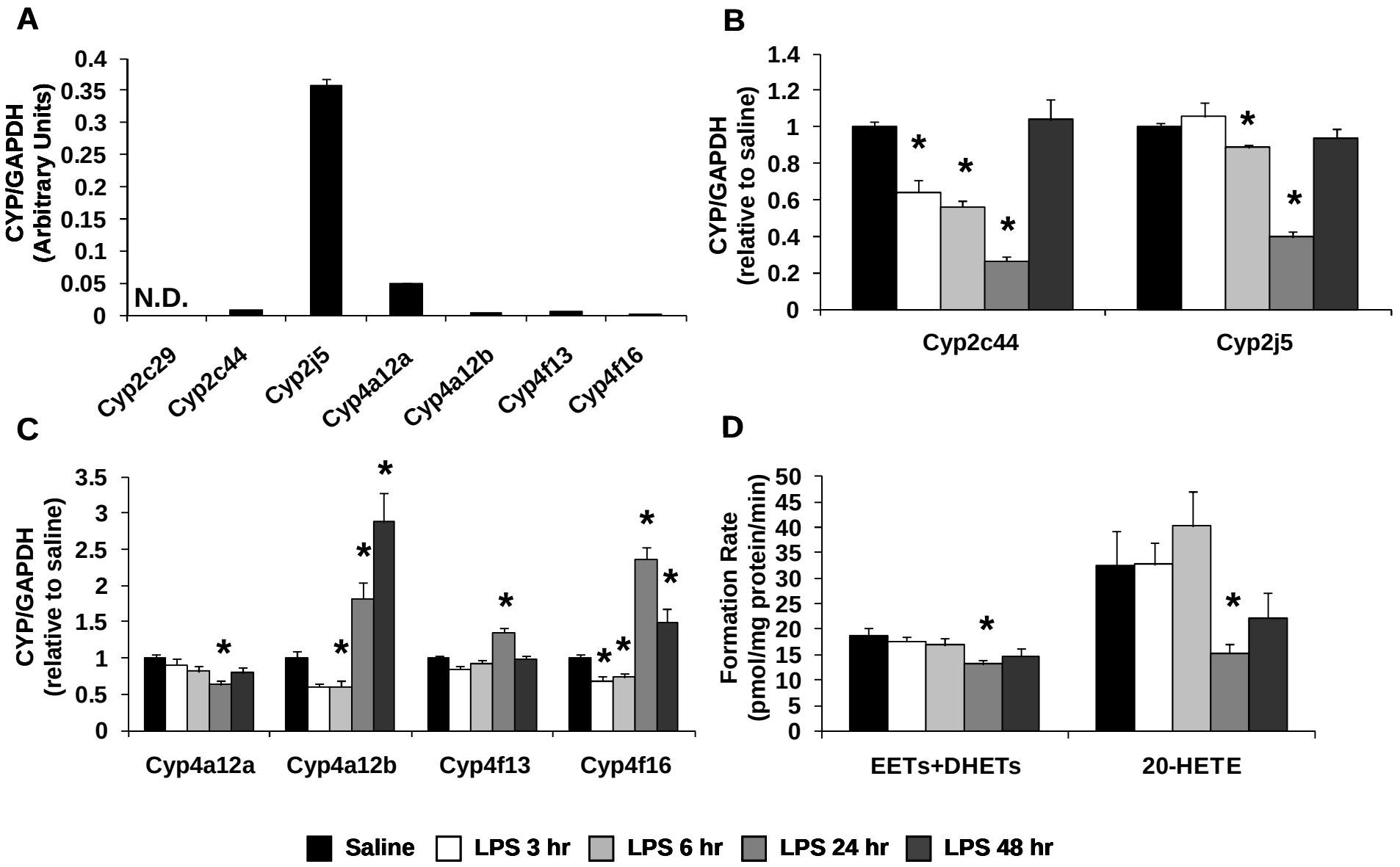

Figure 4: Lung

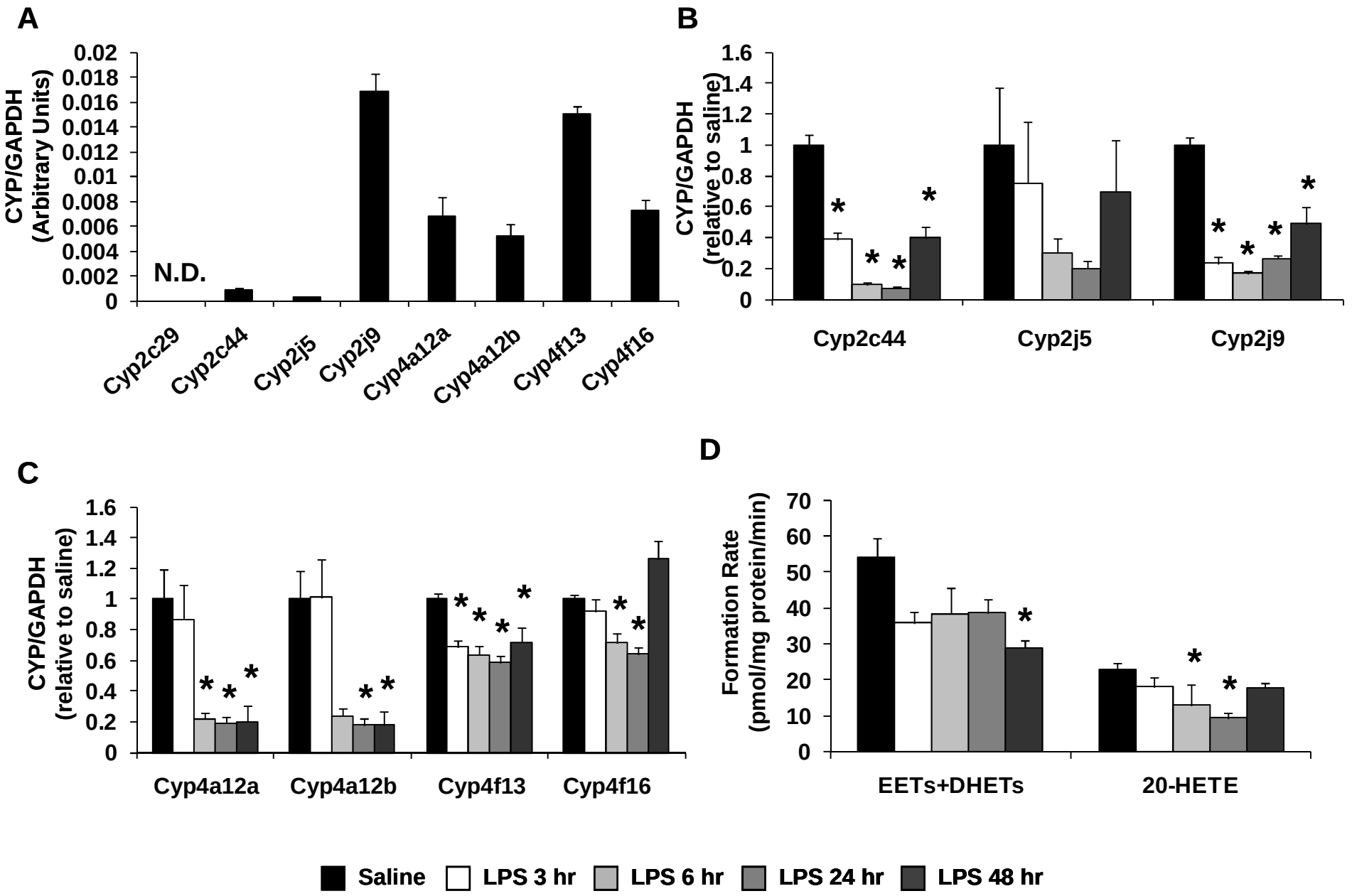

Figure 5: Heart

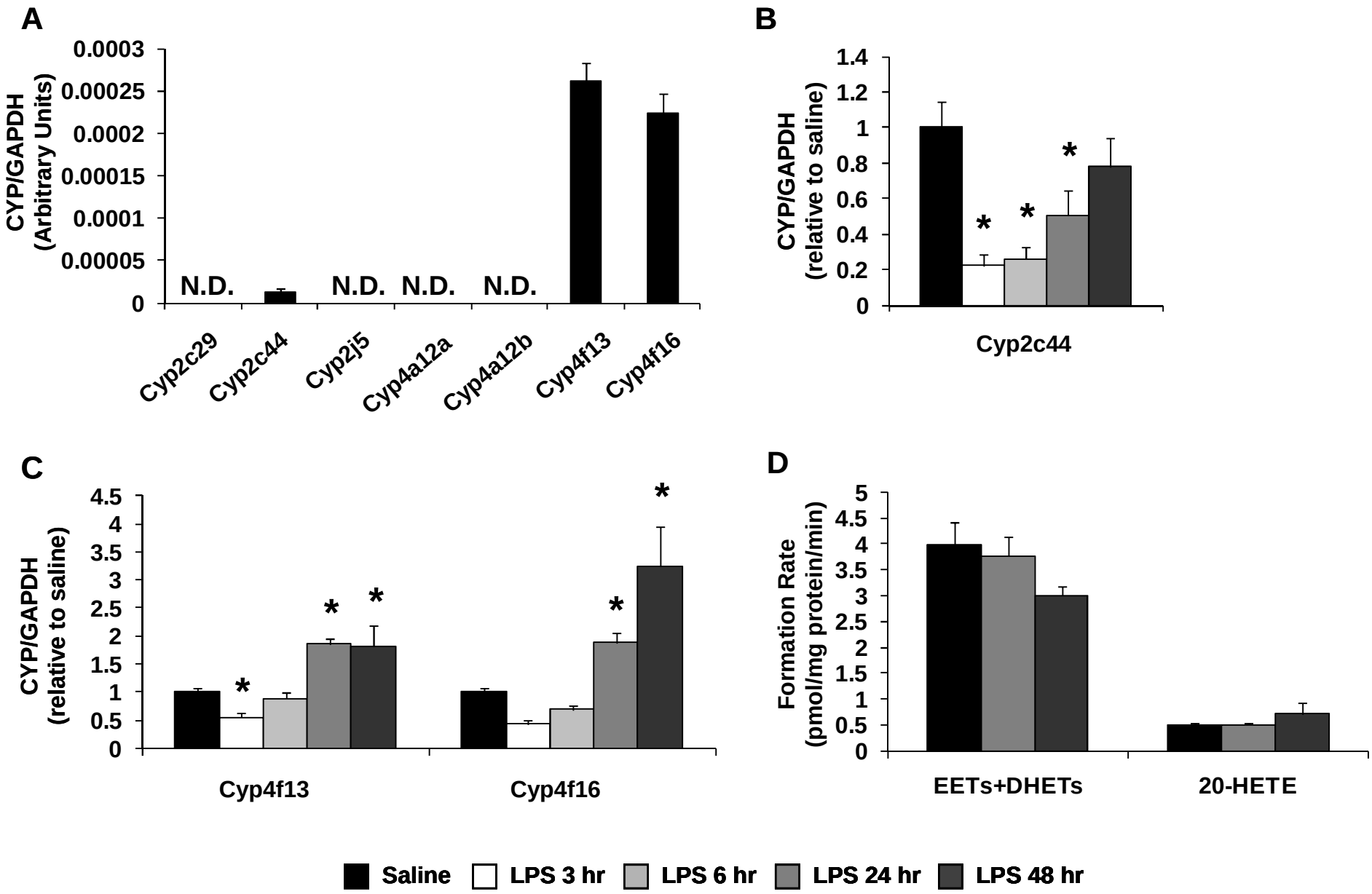

Figure 6

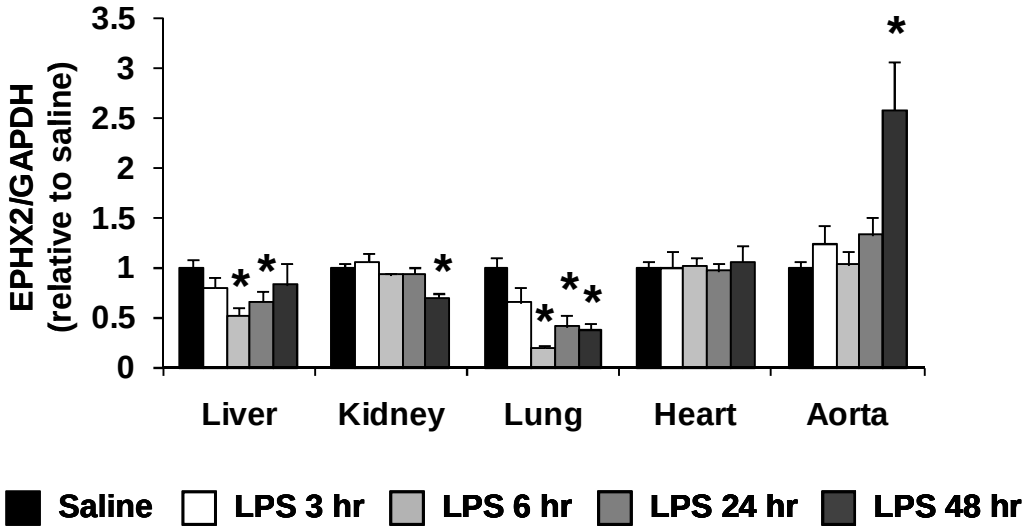

DMD Fast Forward. Published on October 14, 2010 as DOI: 10.1124/dmd.110.035287
This article has not been copyedited and formatted. The final version may differ from this version.

Figure 7

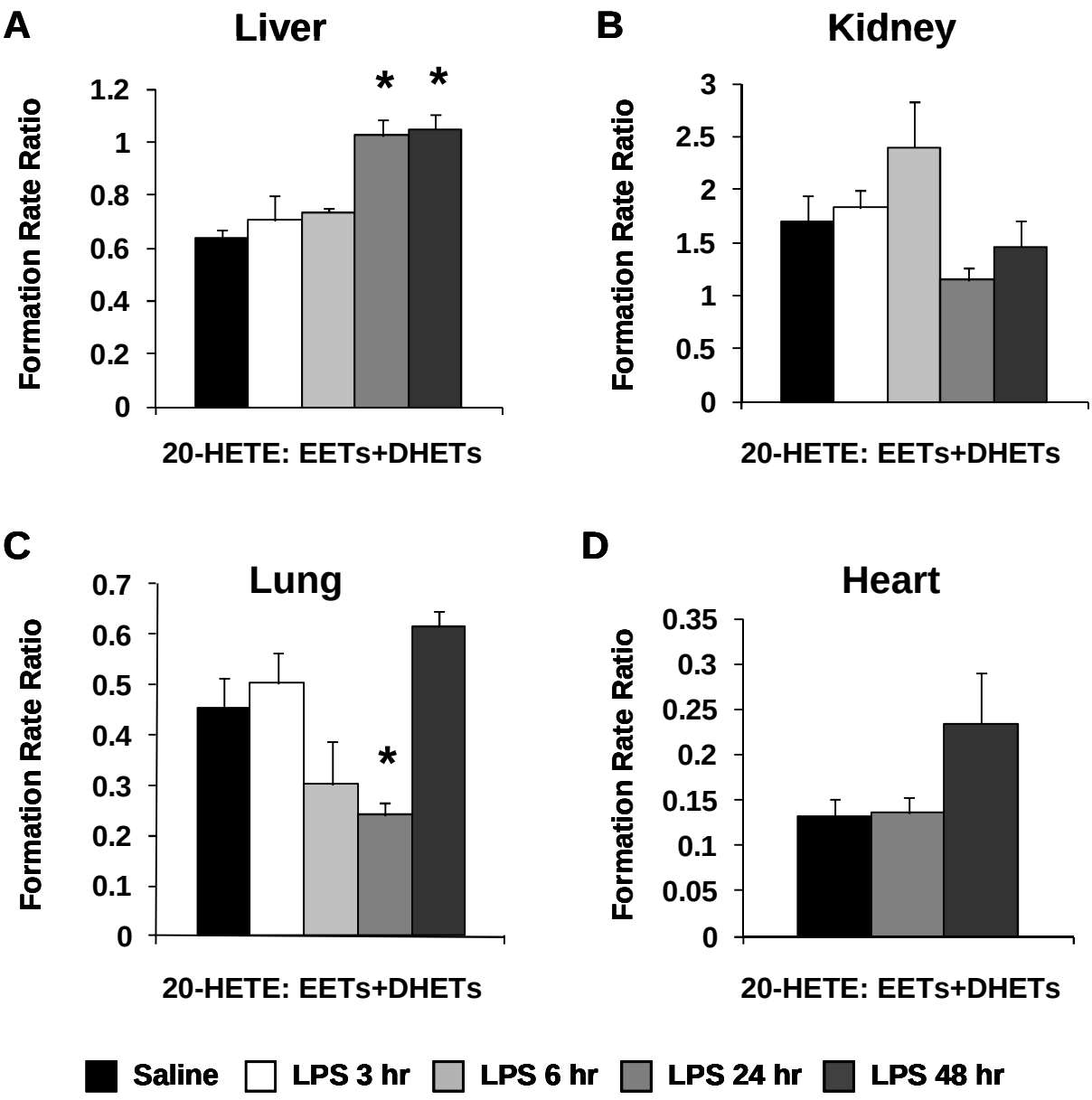

Methods

Immunoblotting

Immunoblotting was performed as previously described (Lee et al.). Briefly, hepatic microsomes (20µg) were separated by electrophoresis using 4-12% NuPAGE Bis-Tris gels (Invitrogen, Carlsbad, CA) and were transferred to nitrocellulose membranes. Membranes were blocked with 5% non-fat milk in Tris-buffered saline (TBS) for 2 hours at room temperature. Membranes were incubated with anti-CYP2C (1:2000 in 5% non-fat milk; kindly provided Dr. Darryl Zeldin, NIH/NIEHS, Research Triangle Park, NC, USA), anti-CYP2J2 pep3 (1:2000 in 5% non-fat milk; kindly provided by Dr. Darryl Zeldin), anti-CYP4A1/2/3 (1:2000 in 5% non-fat milk; Santa Cruz Biotechnology, Santa Cruz, CA), anti-CYP4F2 (1:2000 in 5% BSA, Fitzgerald, Concord, MA), or anti-β-actin (1:1000 in 3% milk, Cell Signaling Technology, Danvers, MA) at 4ºC overnight. The anti-CYP2C antibody was developed against a CYP2C-specific peptide (RGKLPPGPTPLPII) and recognizes multiple murine CYP2C isoforms (Athirakul et al., 2008). The anti-CYP2J2pep3 antibody was developed against a polypeptide (RESMPYTNAVIHEVQRMGNIIPLN) of human CYP2J2 and cross-reacts with murine CYP2J isoforms (Wu et al., 1996). The anti-CYP4A1/2/3 and anti-CYP4F2 antibodies are commercially available polyclonal antibodies that recognize rat CYP4A isoforms and human CYP4F2, respectively. After washing in 0.05% Tween 20-TBS, membranes were incubated with the appropriate horseradish peroxidase-conjugated secondary antibody (1:5000 in 5% non-fat milk; Santa Cruz Biotechnology) for 1.5 hours at room temperature. Immunoreactive bands were detected by chemiluminescence using SuperSignal chemiluminescent substrate (Pierce, Rockford, IL) and visualized with a VersaDoc Imager (Bio-Rad). Densitometry of each immunoreactive band was evaluated using Quantity One software (v.4.4, Bio-Rad).

Plasma Extractions

Plasma (125-200µL) was diluted in 0.12 M potassium phosphate buffer containing 0.113 mM butylated hydroxytoluene, and 12.5 ng 20-HETE-d6 was added as an internal standard. Samples were loaded onto Oasis HLB (30 mg) SPE cartridges (Waters, Milford, MA) that were conditioned and equilibrated with 1 mL of methanol and 1 mL of water, respectively. Columns were washed with three 1 mL volumes of 5% methanol and were eluted with 100% methanol. Extracts were dried under nitrogen gas at 37 ℃ and reconstituted in 125 µL of 80:20 methanol:deionized water.

References

Athirakul K, Bradbury JA, Graves JP, DeGraff LM, Ma J, Zhao Y, Couse JF, Quigley R, Harder DR, Zhao X, Imig JD, Pedersen TL, Newman JW, Hammock BD, Conley AJ, Korach KS, Coffman TM and Zeldin DC (2008) Increased blood pressure in mice lacking cytochrome P450 2J5. *FASEB J* **22:**4096-4108.

Lee CR, Imig JD, Edin ML, Foley J, Degraff LM, Bradbury JA, Graves JP, Lih FB, Clark J, Myers P, Perrow AL, Lepp AN, Kannon MA, Ronnekleiv OK, Alkayed NJ, Falck JR, Tomer KB and Zeldin DC Endothelial expression of human cytochrome P450 epoxygenases lowers blood pressure and attenuates hypertension-induced renal injury in mice. *FASEB J* [May 21, epub ahead of print].

Wu S, Moomaw CR, Tomer KB, Falck JR and Zeldin DC (1996) Molecular cloning and expression of CYP2J2, a human cytochrome P450 arachidonic acid epoxygenase highly expressed in heart. *J Biol Chem* **271:**3460-3468.

Supplemental Table 1: Basal CYP mRNA levels relative to *GAPDH* across tissues.

	Liver	**Kidney**	**Lung**	**Heart**	**Aorta**
Cyp2c29 Mm00725580_s1	0.89 ± 0.10	N.D.	N.D.	N.D.	0.0002 ± 0.0001
Cyp2c44 Mm01197184_m1	0.16 ± 0.01	0.007 ± 0.0003	0.0009 ± $8.3x10^{-5}$	$1.3x10^{-5}$ ± $4.2x10^{-6}$	$7.4x10^{-5}$ ± $3.9x10^{-5}$
Cyp2c50 Mm00663066_gH	0.17 ± 0.03	N.D.	N.D.	N.D.	$3x10^{-5}$ ± $2x10^{-5}$
Cyp2c55 Mm00472168_m1	0.004 ± 0.0002	$1.6x10^{-5}$ ± $1.2x10^{-5}$	N.D.	N.D.	N.D.
Cyp2j5 Mm00487292_m1	0.28 ± 0.03	0.35 ± 0.01	0.0003 ± $7.7x10^{-5}$	N.D.	N.D.
Cyp2j9 Mm00466423_m1	0.0003 ± $2.3x10^{-5}$	0.0006 ± $7.5x10^{-5}$	0.017 ± 0.001	0.0009 ± 0.0002	0.0009 ± $8.4x10^{-5}$
Cyp4a10 Mm02601690_gH	0.04 ± 0.02	0.06 ± 0.01	N.D.	N.D.	$1.3x10^{-5}$ ± $8.6x10^{-6}$
Cyp4a12a Mm00514494_m1	0.21 ± 0.02	0.05 ± 0.002	0.007 ± 0.002	N.D.	N.D.
Cyp4a12b Mm00655431_gH	0.05 ± 0.009	0.003 ± 0.0002	0.005 ± 0.001	N.D.	N.D.
Cyp4f13 Mm00504576_m1	0.02 ± 0.001	0.006 ± 0.0003	0.02 ± 0.0007	0.0003 ± $2.2x10^{-5}$	0.003 ± 0.0002
Cyp4f16 Mm00775893_m1	0.0002 ± $2.9x10^{-5}$	0.0007 ± $4.5x10^{-5}$	0.007 ± 0.0009	0.0002 ± $2.3x10^{-5}$	0.0003 ± $2x10^{-5}$
Ephx2 Mm01313813_m1	0.16 ± 0.02	0.06 ± 0.002	0.004 ± 0.0005	0.02 ± 0.001	0.03 ± 0.002

The commercially available Taqman® Assay on Demand product ID for each gene is provided (Applied Biosystems). Data were generated by quantitative RT-PCR, and are expressed relative to *GAPDH* using the $2^{-\Delta Ct}$ method as mean ± SEM. N=18-24 for all detectable isoforms in each tissue. N.D.= not detected (N=3).

Supplemental Figure 1

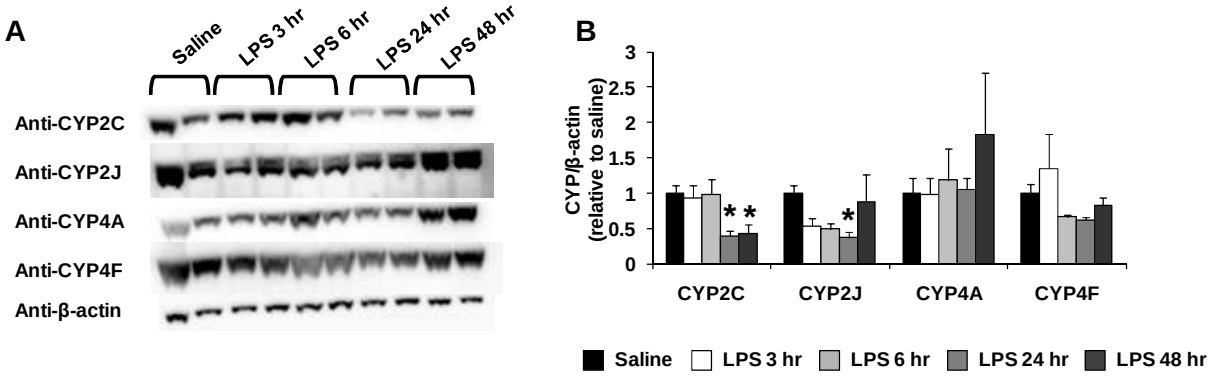

Supplemental Figure 1: (A) Representative immunoblot of CYP and β-actin protein expression in liver microsomes after LPS (1 mg/kg, IP) or saline administration. (B) CYP expression was quantified by densitometry, normalized to β-actin, and expressed relative to the saline control group (Saline: N=8, LPS 3 hours: N=4, 6 hours: N=3, 24 hours: N=8, 48 hours: N=5). * $P<0.05$ versus saline control group.

Supplemental Figure 2

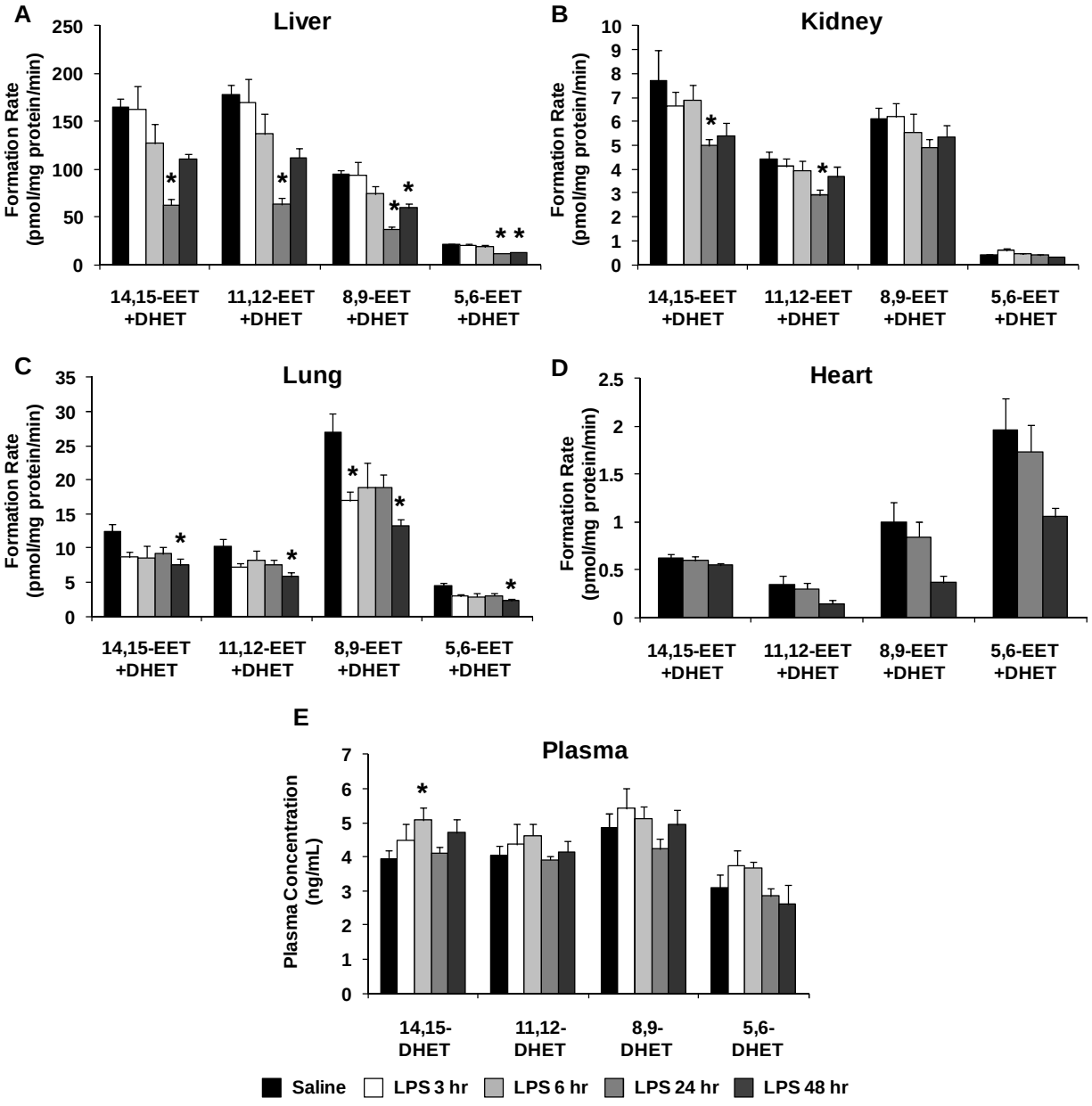

Supplemental Figure 2: The effect of LPS (1 mg/kg, IP) and saline administration on 14,15-, 11,12-, 8,9-, and 5,6-EET+DHET formation was determined in (A) liver, (B) kidney, (C) lung, and (D) heart microsomes [Saline (pooled): N=4-12; LPS 3 hours: N=4-6, 6 hours: N=3-6, 24 hours: N=4-12, 48 hours: N=2-6]. (E) 14,15-DHET, 11,12-DHET, 8,9-DHET, and 5,6-DHET concentrations were quantified in plasma after solid-phase extraction [Saline (pooled): N=17; LPS 3 hours: N=6, 6 hours: N=7, 24 hours: N=15, 48 hours: N=6]. * $P<0.05$ compared to saline-treated mice.